FRACTURE MECHANICS INVESTIGATIONS OF CRACKS IN ROTATING DISCS

M. WENK

Technischer Überwachungs-Verein Norddeutschland e.V., Grosse Bahnstrasse 31, D-2000 Hamburg 54, Germany

SUMMARY

Many engineering constructions such as turbines, pumps or fly-wheels, involve the use of fast rotating components. To optimize their dimensions and to ensure safety in service a precise knowledge of their strength under centrifugal loading is necessary. Conventional methods of assessment are no longer considered to be sufficient when taking into account the increasing demands for reliability of such components, their increasing size and, therefore, increasing potential risk. Recently attempts have been made to apply the methods of fracture mechanics, which have proved successful in solving other problems of strength and safety, to this field as well: ROOKE and TWEED, Int. J. Engng. Sci. 10 (1972), 323; OWEN and GRIFFITH, Int.J. Fracture, 9 (1973) No. 4; ASME safety—guide No. 14; RICARELLLA and BAMFORD, ASME 74-PVP-25 (1974).

These methods should provide a means of determining limiting loads for rotating parts if cracks or cracklike defects are present. In this work the applicability and the limitations of linear elastic fracture mechanics under conditions of centrifugal loading are investigated using the simple case of a rotating solid disc. Stress intensity factors K_I are calculated for radially oriented through-the-thickness cracks as a function of the length and the position at different angular velocities and are measured in model discs using a photoelastic method. In addition, critical stress-intensity factors K_{Ic}^* at the onset of fracture of the model discs are determined in spin burst tests and are compared with values K_{Ic} obtained from static tension tests.

The agreement between the numerically and the experimentally determined stress-intensity factors and between the static and the dynamic critical values ($K_{Ic}^* = K_{Ic}$) confirms the applicability of linear elastic fracture mechanics and the validity of the brittle fracture criterion which says that fracture takes place when $K_I \geq K_{Ic}$. In addition, the results justify the use of a simple superposition procedure to calculate stress-intensity factors as a basis for a strength analysis. The application of these results to practical situations is possible if the assumptions of the linear elastic fracture mechanics are accomplished.

These assumptions require an integral linear elastic behaviour of the precracked component till to the fracture which is veryfied if the loadstresses are small compared with the yield-strength or if the size of the plastic zone at the crack tip is small compared with the thickness. If these assumptions are not accomplished another failure criterion has to be taken. For the geometry and material of a fly-wheel which is used in German reactors at the coolant pumps a failure analysis is done (material: 26 NiCrMo 145 ≙ ASTM A 470 class 7). The fly-wheel is a rotating disc with a bore hole and the stresses are different but this do not injure the applicability of the described concept. With the two failure criterions "fracture if $K \geq K_{Ic}$" and fracture if $\sigma \geq \sigma_y(\sigma_y =$ yield strength) critical angular frequencies are evaluated as a function of the crack length.

1. The Fracture Mechanics Approach

Any fracture mechanics safety analysis requires information from 3 different areas: The local stress distribution in the component (without defects) as a function of geometry and loading as well as the nature, position, shape and size of defects and the actual material behaviour in terms of a fracture toughness parameter must be known (see for instance BLAUEL, KALTHOFF, SOMMER [5]).

The evaluation of the local stresses in a rotating structural part without defects is a straight forward problem of linear elasticity and solutions for a number of simple geometries are available in textbooks. As long as only centrifugal forces are considered the angular frequency ω and the density ρ are the only load parameters.

In general, defects such as for instance inclusions, segregations, pores or cracks arising from material fabrication, production or service conditions cannot be avoided in structural members. If such defects are conservatively approximated by plane cracks (ASME BPV Code Sec. XI) their degradative influence on the structural integrity may be described in a quantitative manner by the stress intensity factors K. These may be determined for the relevant geometry and load parameters if the rotation-induced forces are treated as static (for a constant rate of rotation) and linear elastic material behaviour is assumed. However, the analysis of the rotating part will be complex because the finiteness of the dimensions will play an important role, because the stresses will in general vary along the length of the crack, and because mixed mode conditions will exist for all cracks which are not oriented either radially or axially.

As to the actual material behavior experience from other sorts of strength problems and with different materials leads one to expect that a failure criterion $K_I \geq K_{Ic}$ can also be applied under conditions of centrifugal loading. Accordingly an existing crack in a rotating disc will start to extend in a brittle way if the stress-intensity factor K_I - for an assumed opening mode of loading on the crack - becomes equal to or exceeds a critical threshold value, the fracture toughness K_{Ic}. This is a material constant defining a minimum resistance to fracture propagation and which can be determined independently by laboratory tests. A comparison of the limiting loads in spin burst tests with conventional tension tests should prove the validity of this criterion and provide a sound basis for its applicability to a strength and safety analysis in practical situations.

2. Analytical Determination of Stress-Intensity Factors

The type of specimen chosen as an example for this investigation was a disc of constant thickness without a central hole. The geometry, coordinates and other parameters are shown in fig. 1.

When rotating at a constant angular frequency ω stresses σ_φ and σ_r are generated which are oriented in circumferential and radial direction; σ_φ and σ_r are principal stresses and can be assumed constant through the thickness for $d \ll R$ (TIMOSHENKO and GOODIER [6]):

(1)
$$\sigma_\varphi(r) = \left(\frac{3+\nu}{8} R^2 - \frac{1+3\nu}{8} r^2 \right) \rho \omega^2$$

$$\sigma_r(r) = \frac{3+\nu}{8} \left(R^2 - r^2 \right) \rho \omega^2$$

Here density ρ and POSSION's ratio ν are the only material constants. Fig. 2 shows a numerical evaluation of equ. (1) for the geometry and material conditions of the model experimets described in sec. 3.

As the most critical situation in a structural member (and which can be most easily analyzed) radially oriented trough-the-thickness cracks were investigated. The loading by the circumferential stresses $\sigma_\varphi(r)$ is then of the simple mode I type but it varies along the crack length l and is,in general unsymmetric about the crack center. Here,the method of superposition can be used to evaluate stress intensity factors. For the general situation sketched in fig. 3 one obtains following PARIS and SIH [7]:

(2)

$$K_{Ia} = \frac{\sqrt{2}}{\sqrt{\pi(b-a)}} \int_a^b \sigma_y(x,o) \sqrt{\frac{b-x}{x-a}}\, dx$$

$$K_{Ib} = \frac{\sqrt{2}}{\sqrt{\pi(b-a)}} \int_a^b {}_y(x,o) \sqrt{\frac{x-a}{b-x}}\, dx$$

where K_{Ia} and K_{Ib} are the stress-intensity factors for the crack with one tip at x = a and the other at x = b and $\sigma_y(x,o)$ is the stress distribution along the crack line calculated from the external loading but for the crack free body. For the rotating disc x has to be replaced by r and $\sigma_y(x,o)$ by $\sigma_\varphi(r)$ according to equ. (1):

(3)
$$K_{Ia} = \frac{\sqrt{2}}{8\sqrt{\pi(b-a)}} \rho \omega^2 \int_a^b \left((3+\nu) R^2 - (1+3\nu) r^2 \right) \sqrt{\frac{b-r}{r-a}}\, dr$$

$$K_{Ib} = \frac{\sqrt{2}}{8\sqrt{\pi(b-a)}} \rho \omega^2 \int_a^b \left((3+\nu) R^2 - (1+3\nu) r^2 \right) \sqrt{\frac{r-a}{b-r}}\, dr$$

In the same way as the stresses the stress-intensity factors depend linearly on the density ρ and are proportional to the square of the angular frequency ω ; POISSON's ratio ν comes into the picture in a more complicated way. Basically the stress intensity factors at the two tips of all unsymmetrical cracks are different, with $K_{Ia} \geq K_{Ib}$; only in the central regions $|r| < 0.2R$ they are more or less equal because the stresses are nearly equal. The actual values will depend on the crack length and the locus of the crack center. Equ. (3) has been evaluated numerically and results are shown in figs 8, 9, 10.

The assumption of an infinite region for the deriva tion of equs. (2) and (3) seems to exclude their applicability for situations where either the crack-length is not small compared to the radius of the disc or one of the crack tips is near to the periphery. This would be a consequence of the additional moments induced by the opening crack. But comparing this situation with that of a finite width plate with an edge crack under tension an appreciable reduction of this effect can be expected in the case of the rotating disc due to the higher degree of connectivity. A quantitative measure of this is obtained by comparing our results with those derived from the complete solution of ROOKE and TWEED [1] for the finite width disc. As fig. 4 shows, there is only a difference of less than 8 % for cracks within 80 % of the disc radius; the deviation was found to be of the same sense and of the same magnitude for other crack configurations. For very long cracks or edge-cracks no results of ROOKE and TWEED [8] are available. In the comparison with the experimentally determined stress-intensity factors in the next section only the superposition method results are used.

3. Experimental Determination of Stress-Intensity Factors

To check the analytical results of sec. 2 small scale precracked models made from a suitable transparent material were used. The stress-intensity factors under rotation were determined using a stress optical procedure with stroboscopic illumination.

Fig. 5 shows the experimental arrangement schematically. The disc was held between a point bearing and a trunnion seat both acting on bosses glued to the disc surfaces and it was driven by an infinitely variable electric motor. An opaque marker near the periphery of the disc was used both to determine the rotation frequency and to trigger the light source (Stroboscope Philips PR 9107) through interruption of a light beam incident for the photoelastic system. The other components of the photoelastic system were two polarizing filters with quarter-wave plates, an interference filter for monochromatic light and a camera with a long focal length objective (LEITZ Telyt 1:5, f = 400 mm) to approximate to parallel light illumination.
Fig. 6 shows a series of photoelastic pictures of a crack in a disc rotating at different speeds taken with the above arrangement.

The model discs were made from plates of ARALDIT B (Firma TIEDEMANN, Garmisch-Partenkirchen), a material with a small photoelastic constant ($S = 10.2 \frac{N/mm}{fringe}$) and approximating closely to linear elastic fracture behaviour. The diameter of the discs was $2R = 400$ mm and their thickness $d = 10$ mm. The artificial cracks were saw cuts (0.2 - 0.4 mm wide) which were sharpened with a razor blade.

The evaluation of the fringe pattern at the crack tip relies on the validity of the so-called basic equation of photoelasticity and the linear elastic crack tip stress field equations. The first of these

$$(4) \qquad N = \frac{\Delta s}{\lambda} = \frac{d}{S} = (\sigma_1 - \sigma_2)$$

gives a linear relationsship between the fringe number N - which is the change of optical path length Δs due to the stresses divided by the wavelength λ of the light - and the principal stress difference $\sigma_1 - \sigma_2$ in the loaded specimen; with the photoelastic constant S being the stresses in N/mm^2 required to produce the first isochromatic fringe in a specimen of thickness $d = 1$ mm. The second equation

$$(5) \qquad \sigma_1 - \sigma_2 = \left(\frac{K_I}{4} \sin^2\vartheta - \frac{K_I}{\sqrt{2\pi\rho}} 8a_2 \sin\vartheta \sin\frac{3}{2}\vartheta \right)^{1/2}$$

includes the first terms of a general series-representation in polar coordinates ρ, ϑ of the stresses in the neighbourhood of a crack tip under a pure mode I loading according to IRWIN [9]. The stress-intensity factor K_I and the coefficient a_2 are determined by the boundary conditions of geometry and load. They can be evaluated experimentally by comparing the theoretical lines of constant principal-stress difference according to equ. (5) with the isochromatics described by equ. (4). This fit was accomplished by a numerical regression program of KLEIN [10]. Any one of the isochromatics can be used for such a determination provided that it is not disturbed by the boundary of the disc so that equ. (5) can be applied. For the fitting program it is important to measure very precisely the coordinates ρ_N and ϑ_N along the isochromatic of order N, which is usually a relatively wide fringe. Therefore all negatives of fringe patterns were recopied onto an equal density film (Agfa Contour) which gives two narrow lines from contours of equal density which are symmetrical about the center of an isochromatic fringe. These can then be localized very precisely using a microscope. An example is shown in fig. 7.

Results: In figs. 8, 9, 10 experimentally determined stress-intensity factors K_I for different crack lengths, crack positions and angular velocities of the model discs are compared with theoretical values from equ. (3). For the experimental values the standard deviations is shown which reflects the uncertainties in measuring crack length, coordinates ϱ_N and ϑ_N, and photoelastic constant S and the error from the numerical procedure.

Within the accuracy of the measurements the experimental and theoretical values are in good agreement. The three series of results show that the stress intensity factor at the inner crack tip (as a consequence of the stress distribution) is always greater than at the outer one. Therefore onset of the unstable crack extension can always be expected to occur at the inner crack tip.

Fig. 8 confirms the dependence of K_I on the square of the angular velocity ω. In the lower part of the curve an exact experimental evaluation is no longer possible because the number of fringes is too small.

In the test series of fig. 9 the locus of the outer crack tip had been held constant but the crack length varied. For increasing crack length the risk of unstable fracture also increases and the difference between K_{Ia} and K_{Ib} gets larger. If the position of a crack is varied (see fig. 10) at a constant crack length and a constant angular velocity the stress intensity factors decrease with increasing distance from the center of the disc. In the central part of the disc ($r < 0.2R$) the stress-intensity factors tend towards a constant maximum value.

4. Spin Burst Tests and the Brittle-failure Criterion

To verify the brittle failure criterion that fracture will take place when $K_I \geq K_{Ic}$ a series of cracked model discs were loaded to fracture in spin burst tests. From the limiting angular velocity and the relevant geometrical data of disc and crack a critical stress intensity factor K^*_{Ic} was determined following equ. 3 (using the expression for K_{Ia} since $K_{Ia} \geq K_{Ib}$). Single edge notched specimens were machined afterwards from the broken parts of the discs and were tested according to the recommendations of fracture toughness K_{Ic}-determination (ASTM-Designation E 399-72). Table 1 compares the results of 7 series of tests on ARALDIT B and PMMA specimens.

Taking into account the limited number of tests and the uncertainties of measurement these results show that in the spin burst tests fracture is initiated for all crack positions and crack lengths at a constant material specific value K^*_{Ic} of the stress intensity factor. In addition, table 1 shows that K^*_{Ic} is equal to the staticly determined value K_{Ic}. Therefore it can be concluded that for conditions of centrifugal loading onset of brittle fracture is also determined by the fracture toughness K_{Ic}.

5. Conclusions for a Strength and Failure Analysis

The model experiments using cracked discs of PMMA and ARALDIT B confirm the applicability of the analytical and experimental methods of linear elastic fracture mechanics for centrifugal loading. Therefore, if the same general conditions of material behavior, existence of cracklike defects and state of stress (see sec. 1) are given, these results can be used to analyse real technical situations (see GREENBERG et al [11]). In the following - as an example - the results of sec. 3 and 4 are used to determine the limiting loading of an energy-storage fly-wheel made of steel, which are used at the coolant pumps in german reactors.

The storage wheel is assumed to be a solid disc with a bore hole in the middle (Radius of disc R = 835 mm; radius of bore hole r_o = 275 mm; material 26 NiCrMo 14 5 $\hat{\approx}$ ASTM A 470 Class 7). To obtain a safe limit the following worst assumptions are made for possible defects in the disc: Cracks progagate at the bore hole, go through the full thickness and are radially oriented. The stresses for the disc with a bore hole are (TIMOSHENKO and GOODIER [6]):

$$\sigma_r(r) = \frac{3+\nu}{8}\varrho\omega^2 \left(R^2+r_o^2 - \frac{R^2 r_o^2}{r^2} - r^2\right)$$

(6)

$$\sigma_\varphi(r) = \frac{3+\nu}{8}\varrho\omega^2 \left(R^2+r_o^2 + \frac{R^2 r_o^2}{r^2} - \frac{1+3\nu}{3+\nu}r^2\right)$$

Fig. 11 shows a numerical evaluation of equ. 6 for the geometry and material conditions of fly-wheels used in german reactors. With these stresses you can get the K-factors by the analytical methods of sec. 3. The brittle failure criterions together with the material values ϱ = 7,8 g/cm^3, ν = 0,3, K_{Ic} = 5000 N/mm$^{3/2}$ gets the maximum allowable angular frequencies (see equ. 7), which are plotted in fig. 12 as a function of crack length.

(7) $$\omega_c^2 = K_{Ic} \left(\frac{\sqrt{2}(3+\nu)}{8\sqrt{\pi l}} \cdot \varrho \int_{r_o}^{r_o+l} \left(R^2+r_o^2 + \frac{R^2 r_o^2}{r^2} - \frac{1+3\nu}{3+\nu} r^2\right)\sqrt{\frac{r_o-r}{r-(r_o+l)}}\,dr\right)^{-1}$$

The dashed and dotted line shows a very conservativ method to evaluate the maximum allowable angular frequencies by taking a constant stress along the radius between r_o and R. Here you can see the advantage of the superposition method which considers the real stress conditions in the fly-wheel.

The linear elastic fracture mechanics approach, i.e. sec 2 is no longer valid if the material yield stress σ_y is exceeded in larger areas of the disc. Then the disc will fail by plastic collapse independently of crack length at a critical angular frequency

$$\omega_c = 2\sqrt{\frac{\sigma_y}{(3+\nu)R^2+(1-\nu)r_o^2}} \tag{8}$$

This limit is also shown in fig. 12. Thus the maximum allowable angular frequency is determined by either equ. (7) or (8) depending on which one gives the smaller value of ω_c. This then, in turn, determines the maximum amount of kinetic energy

$$E_{max} = \frac{1}{4}\pi\left(R^4-r_o^4\right) \, d\,\varrho\,\omega_c^2 \tag{9}$$

which can be stored in such a disc.

6. Acknowledgement

The work on which this publication is based formed part of an investigation by the firm of Maschinenfabrik Augsburg-Nürnberg (MAN) into the possible use of fly-wheels for energy storage. This investigation was funded by the Bundesminister für Forschung und Technologie (BMFT) of the Federal Republic of Germany. The BMFT accepts no responsibility for the correctness, accuracy and completeness of this work nor any liability fot the rights of third parties.

References

[1] ROOKE, D. P., TWEED, J.,"The Stress-Intensity Factors of a Radial Crack in a Finite Rotating Elastic Disc", Int. J. Engng. Sci. 10 (1972), pp. 323 - 335.

[2] OWEN, D. R. J., GRIFFITHS, J. R., "Stress-Intensity Factors of Cracks in a Plate Containing a Hole and in a Spinning Disc", Int. J. of Fracture, Vol. 9, Nr. 4 (1973).

[3] RICARDELLA, P. C., BAMFORD, W. H., "Reactor Coolant Pump Flywheel Overspeed Evaluation", ASME 74-PVP-25 (1974).

[4] WENK, M. "Bruchmechanische Untersuchungen zum Festigkeitsverhalten von rißbehafteten rotierenden Scheiben", Diploma-Thesis, Univ. Freiburg (1975).

[5] BLAUEL, J. G., KALTHOFF, J. F., SOMMER, E., "Die Bruchmechanik als Grundlage für das Verständnis des Festigkeitsverhaltens", Materialprüfung 12 (1970) Nr. 3, 69 - 76.

[6] TIMOSHENKO, J., GOODIER, J. N., "Theory of Elasticity", McGraw Hill, New York (1965).

[7] PARIS, P. C., SIH, G. C., "Stress Analysis of Cracks", ASTM Spec. Techn. Publ. No 381 (1965), 30 - 83.

[8] ROOKE, D. P., TWEED, J., "The Stress-Intensity Factors of an Edge Crack in a Finite Elastic Disc", Int. J. Engng. Sci. 11 (1973), pp. 65 - 73.

[9] IRWIN, G. R., "Analysis of Stress and Strains Near the End of a Crack Traversing a Plate", Trans. ASME, J. Appl. Mech. 24 (1957), 361 - 364.

[10] KLEIN, G., "Bestimmung von Spannungsfaktoren bei gemischten Beanspruchungsarten am Beispiel eines Risses in der Umgebung eines Kreislochs", Diss. Karlsruhe (1974).

[11] GREENBERG, H. D., WESSEL, E. T., PRYLE, W. H., "Fracture Toughness of Turbine Generator Rotor Forgings", Eng. Fract. Mech. 1 (1970), 653 - 674.

Table 1: Comparison of critical stress-intensity factors K^*_{Ic} and K_{Ic} for ARALDIT B and PMMA determined in spin burst tests using equ. (3) and by conventional fracture toughness tests under pure static tension (the numbers in brackets are the numbers of tests; specimen thickness in all cases d = 5 mm)

	radial crack		"dynamic" test		"static" test
material	a	l	ω crit	K^*_{Ic}	K_{Ic}
	mm	mm	sec^{-1}	$N/mm^{3/2}$	$N/mm^{3/2}$
Araldit B	100	15	$77 \cdot 2\pi$	24.5(5)	
Araldit B	90	25	$72 \cdot 2\pi$	27.4(5)	
					25 ± 6 (20)
Araldit B	80	35	$65 \cdot 2\pi$	27.3(5)	
			mean value	26 ± 4	
PMMA	60	20	$97 \cdot 2\pi$	39.1(5)	
PMMA	90	20	$103 \cdot 2\pi$	41.6(5)	
					46 ± 12 (10)
PMMA	110	20	$112 \cdot 2\pi$	44.4(5)	
PMMA	130	20	$119 \cdot 2\pi$	45.7(5)	
			mean value	43 ± 10	

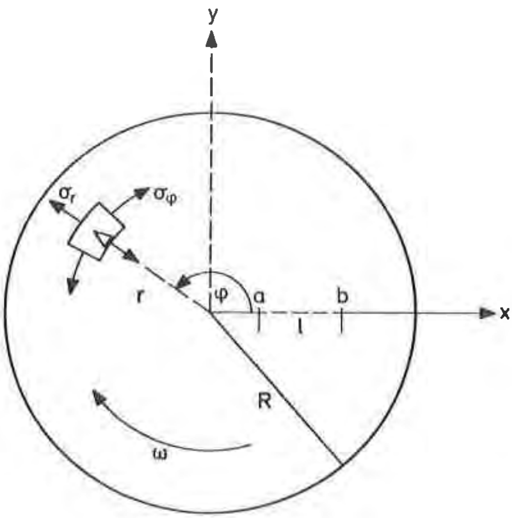

Fig. 1:

Geometry, coordinates and other parameters of the rotating disc
R = external Radius; d = thickness with $d/R \ll 1$; x,y = CARTESIAN coordinates; r,φ = polar coordinates; a,b = tips of a radially oriented through-the-thickness crack; b - a = l = crack length; ω = angular frequency; σ_r, σ_φ = radial and circumferential stresses

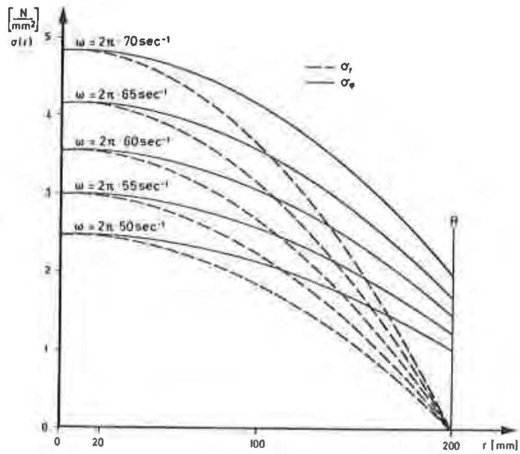

Fig. 2:

Radial σ_r and circumferential stresses σ_φ in a rotating disc
R = radius of disc = 200 mm; material: ϱ = 1,5 g/cm^3, ν = 0,33 (PMMA or ARALDIT B); ω = angular frequency [rps]

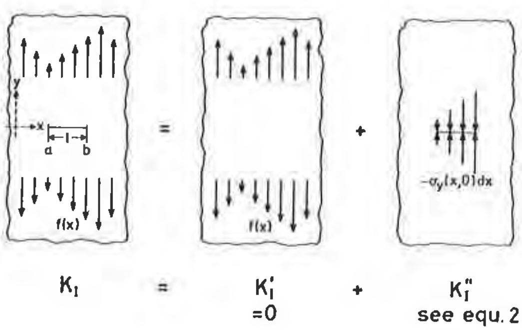

Fig. 3:

Principle of the method of superposition
f (x) = given distribution of external forces. l = b-a = crack length; σ_y(x,0) = distribution of stresses in the crack free body induced by the external forces f (x) along the prospective crack line; - σ_y(x,0)dx = distribution of forces acting along the crack line to induce stress-free boundaries by superposition to the forces due to the stresses σ_y (x,0)

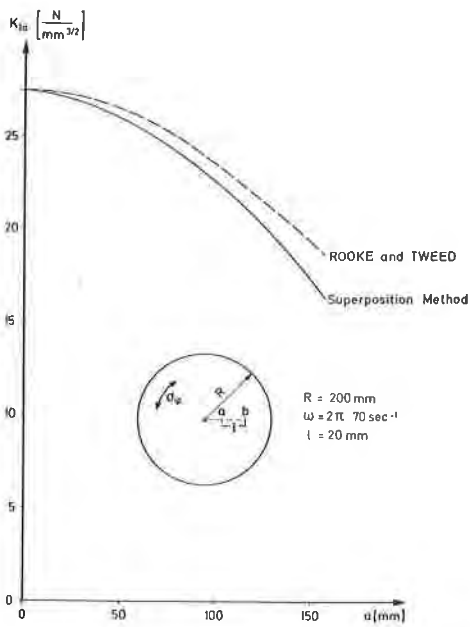

Fig. 4:

Comparison of results from the superposition method and the solution of ROOKE and TWEED (1972)
K_{Ia} = stress-intensity factor for the inner tip of a radial crack of length b-a = l = 20 mm in a disc. (radius R = 200 mm, ϱ = 1,5 g/cm^3 ν = 0,33) under centrifugal loading ω = 2π · 70 s^{-1}

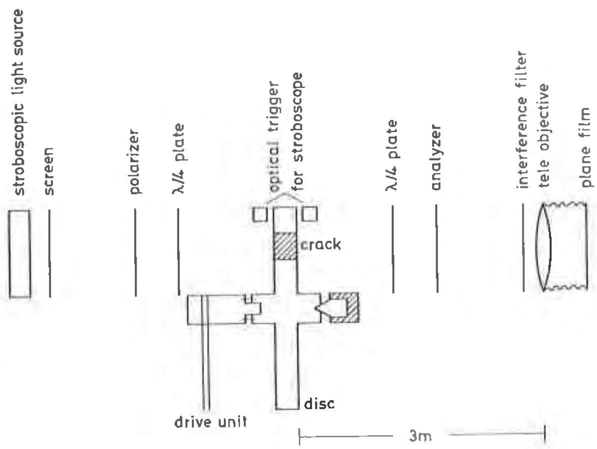

Fig. 5: Schematic sketch of the arrangement for the photoelastic determination of stress intensity factors in a rotating cracked disc

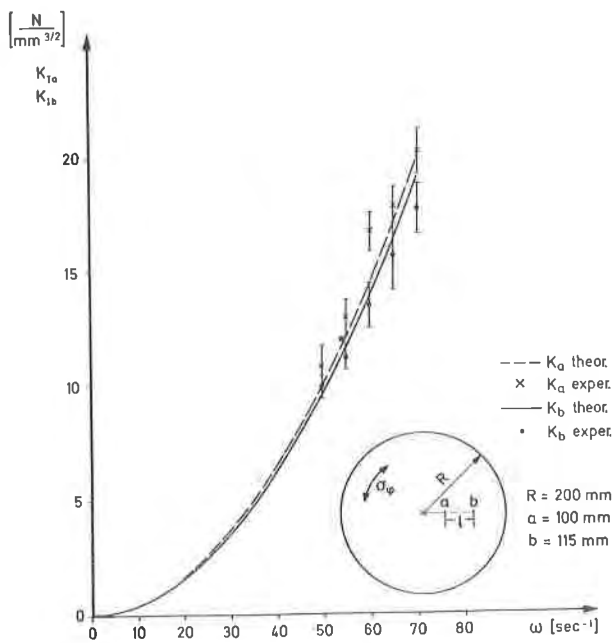

Fig. 6: Measured and calculated stress-intensity factors K_I for a crack of length l = 15 mm in a rotating disc of ARALDIT B (R = 200 mm, ϱ = 1,5 g/cm^3, ν = 0,33) as a function of angular frequency

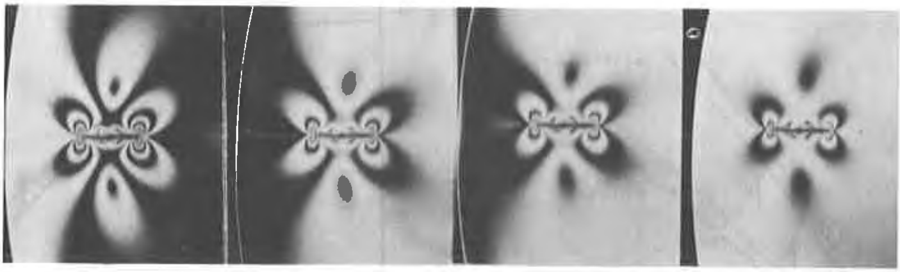

$70\ sec^{-1}$ $65\ sec^{-1}$ $60\ sec^{-1}$ $50\ sec^{-1}$

Fig. 6: Isochromatic fringe patterns of a crack in a rotating disc at different angular frequencies
material: ARALDIT B; thickness of disc d = 10 mm,
radius R = 200 mm, crack length l = 13 mm,
inner crack tip at a = 162,5 mm

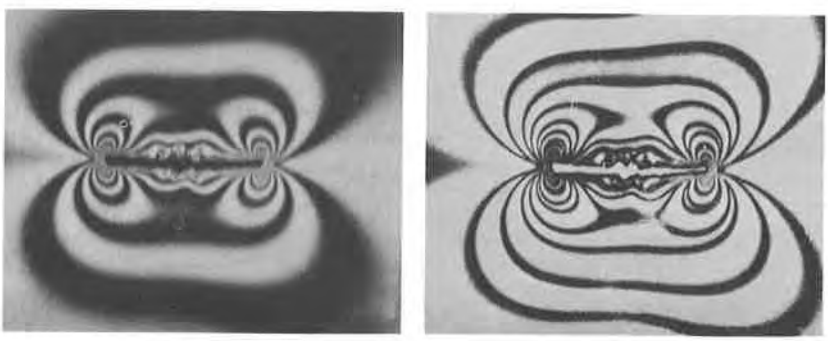

Fig. 7: Isochromatic fringes around a radial crack in a rotating disc together with the corresponding patterns of equal density contours
disc: ARALDIT B, R = 200 mm, d = 10 mm; crack: a = 100 mm
l = 15 mm, $= 2 \cdot 65\ s^{-1}$

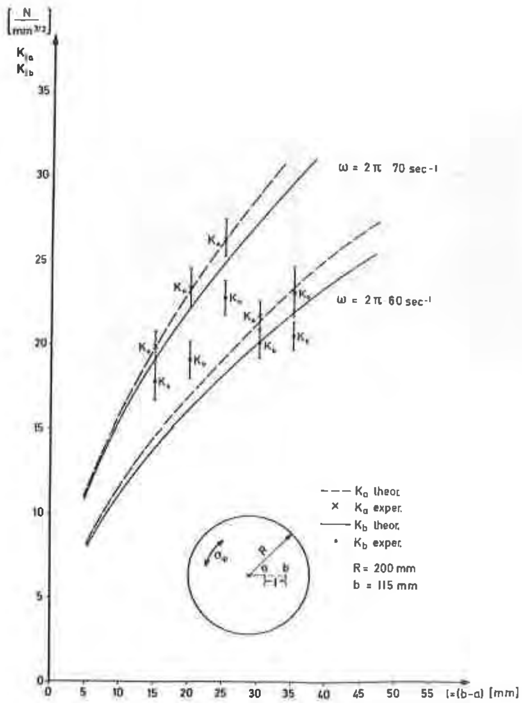

Fig. 9:

Measured and calculated stress-intensity factors for 5 different crack lengths l = b-a at two different angular velocities ; material: ARALDIT B

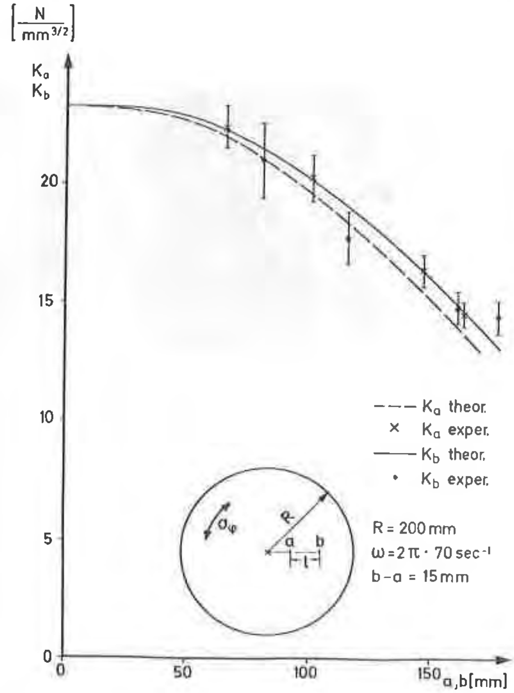

Fig. 10:

Measured and calculated stress-intensity factors for cracks of constant lengths l = b-a = 15 mm but different distances from the center of the disc rotating at $\omega = 2\pi \cdot 70\ s^{-1}$; material: ARALDIT B

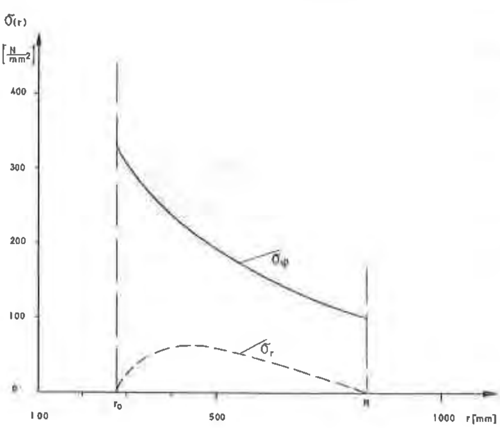

Fig. 11:

Radial σ_r and circumferential stresses σ_φ in a rotating disc with a bore hole in the middle of the disc.
R = radius of disc = 835 mm; r_o = radius of the bore hole = 275 mm; material constants: $\rho = 7{,}5\ g/cm^3$ $\nu = 0{,}3$ (26 NiCrMo 14 5)
ω = angular frequency (42 r/ps`)

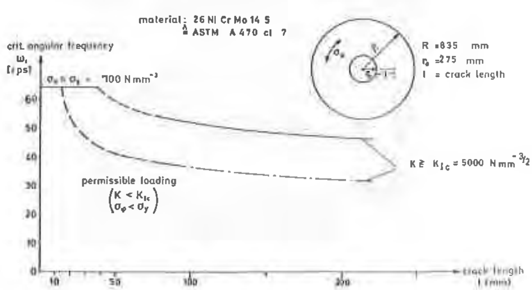

Fig. 12:

Maximum allowable angular frequencies for an energy-storage flywheel made of 26 NiCrMo 14 5 ≙ ASTM A 470 class 7 as a function of crack length l